COMBINED ANALYSIS OF NUCLEAR DATA AND PARTICLE MASSES. II

S.I. Sukhoruchkin , M.S. Sukhoruchkina

Petersburg Nuclear Physics Institute NRC "Kurchatov Institute" 188300 Gatchina

1. Introduction

Neutron resonance spectroscopy is part of Nuclear Physics, and they both play an important role in the development of the Standard Model (SM) - a theory of all interactions except gravitation, with a representation of its components [1,2]:

$$SU(3)_{col} \otimes SU(2)_L \otimes U(1)_Y. \tag{1}$$

A recent analysis of particle masses [3-5] confirmed the existence of the period $\delta = 16m_e$ introduced in [6], as well as unexpectedly accurate empirical relations between the nucleon masses and the electron mass. It was based on the exactly known ratio m_n/m_e=1838.6836605(11) of the neutron mass to the electron mass and the nucleon mass splitting δm_N=1293.3322(4) keV. The neutron mass shift from 115·16m_e - m_e is δm_n = 161.6491(6) keV, exactly 1/8 of δm_N. The ratio $\delta m_N : \delta m_n$ =8.00086(3)≈8×1.0001(1) allows us to represent the nucleon mass ("CODATA relations"):

$$m_n = 115 \cdot 16m_e - m_e - \delta m_N/8 \qquad m_p = 115 \cdot 16m_e - m_e - 9(\delta m_N/8). \tag{2}$$

The shift δm_n coincides with the parameter of tensor forces Δ^{TF}=161 keV, found in the excitations of nuclei where the one-pion exchange dynamics dominates [7,8]. The ratio of the δm_n=Δ^{TF} to pion mass $\delta m_n/m_\pi = 115.86 \cdot 10^{-5}$ is very close to QED radiative correction $\alpha/2\pi = 115.96 \cdot 10^{-5}$ (see 2nd line in Table 1). R. Feynman [9], V. Belokurov and D. Shirkov [10] considered the appearance of the radiative correction as an indication on the important role of the influence of physical condensate on the particle mass.

The CODATA relations (2) mean the presence of two fine structures in the nucleon mass representation: the first, connected with the electron mass m_e (shift is -m_e/3=170 keV in addition to the period $16m_e = \delta$), and the second, with parameter 161 keV=Δ^{TF}=δm_N/8. Both parameters are connected by the factor $\alpha/2\pi$ with the value of the nucleon Δ-excitation ΔM_Δ=147 MeV=(m_Δ-m_N)/2 (the parameter of the Nonrelativistic Constituent Quark Model NRCQM, based on pion-like interaction) [11-13] and with the pion mass 140 MeV=$m_{\pi^\pm}$ itself (Table 1). The initial mass of the baryon constituent quark in NRCQM is three times ΔM_Δ, namely, M_q=441 MeV=m_Ξ/3. The mass of the meson constituent quark M_q'' in NRCQM is derived as a half the masses of ω and K^* mesons close to 780 MeV=6f_π where f_π=130.7 MeV=16δ is the pion β-decay parameter. The period f_π=16δ=M_q''/6 was used in the two-dimensional representation of particle masses (in Fig. 1), where the integers of the other NRCQM parameters $m_\pi = (16+1)\delta$ and $\Delta M_\Delta = M_q/3 = (16+2)\delta$ are represented as straight lines.

The important role of both NRCQM parameters $M_q = 3 \times 18\delta$ and $M_q'' = 3 \times 16\delta$ (presented in Table 2 under the corresponding numbers 16·16 and 16·18) is seen from empirical relations, starting with the proximity to $\alpha/2\pi$ of the ratio of the NRCQM parameter ΔM_Δ=147 MeV to the mass of the scalar field M_{H°=125 GeV (last column in Table 2, line 11 in Table 1). NRCQM provides very accurate (within about 8 MeV) calculations of baryon masses. In combination with CODATA relations and QED radiative correction, confirmed by neutron resonance data (Table 1 bottom), this provide the basis for the SM development.

Table 1. Comparison of the parameter $\alpha/2\pi$=115.96·10^{-5} with the anomalous magnetic moment of the electron $\Delta\mu_e/\mu_e$ (top line), the ratio 1/(32×25)=115.74·10^{-5} and ratios between the mass/energy values considered in the text (four important relations are boxed) [3-5,14-16].

No.	Parameter	Components of the ratio	Value $\times 10^5$
1	$\Delta\mu_e/\mu_e$	$=\alpha/2\pi$-0.328 α^2/π^2	$\boxed{115.965}$
2	$\delta m_n/m_\pi$	$\boxed{(\mathrm{k}\times m_e\text{-}m_n)/m_\pi=161.649\,\mathrm{keV}/m_\pi}$	$\boxed{115.86}$
3	$\delta m_\mu/m_\mu$	$(23\times 9m_e\text{-}m_\mu)/m_\mu$	112.1
4	m_μ/M_Z	$\boxed{m_\mu/M_Z=91182(2)\,\mathrm{MeV}}$	$\boxed{115.87(1)}$
5	$\delta(\delta m_\pi)/9m_e$	$\boxed{(\Delta\text{-}4593{,}66(48)\,\mathrm{keV})/(9m_e=\Delta)}$	116(10)
6	m_d/m_b	m_d=4.78(9) MeV/ m_b=4.18(3) GeV	114
7	m_u/m_c	m_u=2.2(5) MeV/ m_c=1275(25) MeV	173(40)
8	$\varepsilon''/\varepsilon'$	1.35(2) eV/1.16(1) keV	116(3)
9	$\varepsilon'/\varepsilon_o$	1.16(1) keV/ε_o=1022 keV	114(1)
10	$\varepsilon_o/2M_q \approx 1/(32\times 27)$	10 $\varepsilon_o/3(m_\Delta\text{-}m_N)=(\varepsilon_o/6)/\Delta M\Delta$	116.02
11	$(\Delta M_\Delta=M_q/3)/M_{H^\circ}$	147 MeV/125 GeV	118
12	Sb, D(187 eV)/161 keV	(373 eV/2=187 eV)/160 keV, Table 3	114
13	Pd, D(1497 eV)/1293 keV	Fig. 3, Fig. 4 bottom	115.7
14	Hf, $D(1501\,\mathrm{eV})/\delta m_N$	^{172,176}Hf $E^*(0^+)$=1293 keV=δm_N	116.1
15	Os, $D(1198\,\mathrm{eV})/2m_e$	^{178,180}Os $E^*(0^+)$=1023 keV=$2m_e$	117

Evolution of the nucleon mass from the initial value of $3M_q = m_\Xi$ (N=$9\times 18\delta = 162\delta$, Fig. 1, top) to the deuteron mass Δ, corresponding to N=151-150 in units of $\delta = 16m_e$ and the constituent quark $M'_q = 50\delta$, directly seen as the equidistancy in masses of pseudoscalar mesons (shown in Fig. 1, bottom), means the transition of $\Delta M_\Delta(N = 18)$ in m_π or f_π (N=17,16). The final stage of nucleon mass evolution (the mass of about 940 MeV-8 MeV-932 MeV) is situated close to $6f_\pi + \Delta M_\Delta$ (circled point in Fig. 1). It corresponds to the important role of parameters f_π and $3f_\pi \approx M''_q$ in the particle mass spectrum (N=16·16, in the central column of Table 2).

The two lightest particles, the electron and the muon, correspond to the last SM component (1). Their masses are in a ratio of m_μ/m_e=105.65937 MeV/510.9983 keV=206.77 which slightly deviates (difference=0.232) from the integer value L=207=13×16-1 (lepton ratio) by a small factor of 112.08·10^{-5} (the ratio of the difference to L), close to QED radiative correction $\alpha/2\pi = 115.96\cdot 10^{-5}$ (lines 1 and 3 of Table 1). The ratio of the muon mass to the important SM parameter - the vector boson mass $m_\mu/(M_Z$=91.1816(21) GeV)=115.87·10^{-5} is very close to $\alpha/2\pi$ (4th line of Table 1). The difference 1566.70 MeV between the mass of heavy lepton m_τ=1776.82 MeV and two muon masses 210.12 MeV is close to 1569.79=4×48δ=4×392.45 MeV (or to four constituent quarks $M''_q = m_\rho/2$=388 MeV and the value of 1565.30 - the doubled value of $m_\omega/2$=782.65 MeV=2×391.3 MeV).

The relations between the existing estimates of the quark masses (m_u, m_d, m_c, m_b) and the proximity of the splitting of the pion mass to $9m_e$ are presented in lines 5, 6 and 7. In the central part of Table 1 (lines 8-11), the ratios obtained previously [6] between different structures in nuclear excitations and in the particle mass spectrum (superfine period ε''=1.35 eV=5.5 eV/4=δ'/8=11 eV/8, fine structure period ε'=1.16 keV=δ'/8=9.5 keV/8, $\varepsilon_o = 2m_e$=1.022 MeV and M_q=441 MeV=3ΔM_Δ) are given [3-5,14-16] together with the important parameter SM M_{H° (mass of the scalar field) and the ratios between the nuclear intervals considered in this work (Table 1, lines 13-16, and Table 2).

The empirical correlations in particle masses discussed here relate to the role of lepton masses (m_e, m_μ, m_τ) together with the NRCQM parameters and the presence of integer relations 1:13:16:17:18:48:54=δ:m_μ:f_π:m_π:ΔM_Δ:M''_q:M_q with the period of $16m_e = \delta$=8.176 MeV close to the doubled value of the pion β-decay energy]6]. The value $M_q = m_\Xi/3$ (baryon constituent quark mass), as well as M''_q are interconnected with masses of quarks and fundamental fields. In Table 2 they are compared with the numbers of fermions in the central field. Additionally, ratios between them and both vector boson masses, namely, M_Z/M_q=206.8 and M_W/M''_q=207.3 ($M''_q = m_\rho/2$=387.6 MeV) are close to the lepton ratio L=m_μ/m_e=207=16×13-1. This can be considered together with other symmetry motivated relations, including a 16:1 ratio between the period $\delta = 16m_e$ and $m_e = 3 \cdot (m_e/3)$, with m_e observed directly as a shift in the nucleon mass corresponding to a shift of $3(m_e/3)$ in the mass of each of three baryon quarks. Number 16 (for N=16 in Table 2) could be assigned to particle-hole configuration, schematically, 16=16-1+1 [3-5].

Table 2. Comparison of numbers of fermions in the central field (top line) with ratios between the masses m_e/M_q, m_μ/M_Z, $f_\pi/((2/3)m_t = M'_H$ (with m_t and M'_H - masses of top quark and unconfirmed scalar [1,3-5]), $\Delta M_\Delta/M_{H^0}$ and QED parameter $\alpha/2\pi$. Boxed in the bottom line are the hole configuration in $1p$ shell (configuration $1s^4_{1/2}$, $1p^8_{3/2}$, $1p_{1/2}$) and the valence fermion configuration as a fermion with the new principal quantum number over the filled shells (configuration $1s^4_{1/2}$, $1p^8_{3/2}$, $1p^4_{1/2}$).

N^{ferm}	N = 1	N=16	$\boxed{\text{16·13-1=L}}$	16·16	$\boxed{\text{16·17+1}}$	16·18
Const. quark				$M''_q = 3f_\pi$		$M_q = 3\Delta M_\Delta$
Particle mass	m_e	δ	m$_\mu$	f_π	$m_{\pi^\pm}$	ΔM_Δ
Particle/param.	m_e/M_q		m$_\mu/M_Z$	$f_\pi/((2/3)m_t)$		$\Delta M_\Delta/M_{H^0}$
Ratio	115.96·10^{-5}		115.87·10^{-5}	114·10^{-5}		117·10^{-5}
Comments			$\boxed{\text{hole in } 1p}$	filled shells	$\boxed{\text{valence}}$	

To check the periodicity with the parameter δ, all existing data from the PDG compilation were used, and distributions of differences between the masses of all particles known with an uncertainly of less than 8 MeV were plotted (ΔM in Fig. 2). The maximum at ΔM=m_π=142 MeV in this distribution (Fig. 2), the doublet of maxima at ΔM=1671-1687 MeV (including $12m_\pi = m_\Omega$) and the maximum at ΔM=3370 MeV=$24m_\pi$ correspond to distinguished stability of intervals with N=17 (numbers of the period $\delta = 16m_e$). The period $\delta = 16m_e$ manifested also as stable splittings of 17 MeV=2δ and 48 MeV=6δ in the same Fig. 2 (top). Stable intervals with ΔM=445 MeV and 462 MeV are close to M_q=441 MeV, the main parameter of NRCQM model. The doublet at ΔM=3940-3959 MeV is close to $9M_q$=3963 MeV. The value of 932 MeV=$6f_\pi$+ΔM_Δ coincides with the nucleon mass in nuclear media (the final stage of nucleon mass evolution). The doublet at 1671-1687 MeV = $12m_\pi$ and the maximum at exactly two-fold energy 3370 MeV = 24m$_\pi$ corresponds to the observed empirical periodicity (with the interval m_π) in masses of $\Lambda-, \Xi-, \Omega$-hyperons and the charmed quark mass m_c (k=1, 8, 9, 11, 12 of the period m_π [3-6,14-16]). Splitting in all doublets observed in Fig. 2 is about 17 MeV=2δ

including the doublets at ΔM=3959 MeV=9M$_q$ and 4425 MeV=10M$_q$. This means the existence of small splitting with a common value 2δ=17 MeV and long-range correlations with the parameter $M_q = 3\Delta M_\Delta$ (k=1, 9, 10, with $\Delta M_\Delta = 18\delta$) and the pion mass m$_\pi$=142 MeV=17$\delta$.

The direct manifestation of the pion mass ($m_{\pi^\pm}$=139.57 MeV) in the spectrum of charmed hadrons was noticed by G. Mac Gregor [17]: three values coincide within 1 MeV, namely, $D^{*\pm}-D^\pm$=140.7 MeV, $D_s^{*\pm}-D_s^\pm$=141.6 MeV and $\chi_{C2}(1P)-\chi_{C0}(1P)$=141.2 MeV. The ratios 1:12:24=m_π:12m_π:24m_π between the positions of the maxima in the ΔM distribution are in agreement with the coincidence of the charmed quark m_c=1275(25) MeV with $9m_\pi$=1255 MeV (shown in Fig. 1 as m_c on the straight line $k \cdot m_\pi$).

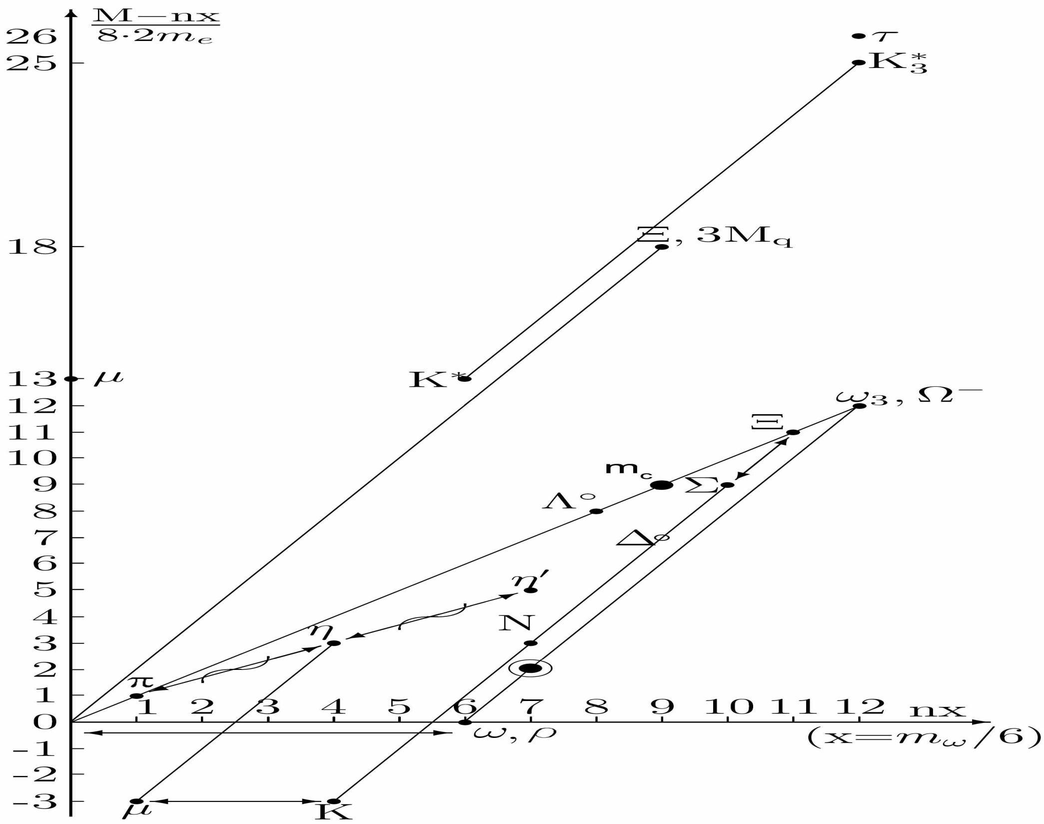

Fig. 1. Evolution of the baryon mass from $3M_q$ to nucleon mass M_N is shown in two-dimensional presentation: values in the horizontal direction are in units $16 \cdot 16m_e = f_\pi$=130.7 MeV, remainders M_i-n$(16 \cdot 16m_e)$ are plotted along the vertical axis in units of $16m_e$. Nucleon mass in nuclear medium (circled point) is close to the sum ΔM_Δ+6f_π. Both parameters, $f_\pi = M''_q/3 = M_w/3L$ and $\Delta M_\Delta = M_q/3 = M_Z/3L$, are connected with the fundamental fields and with the CODATA period $\delta = 16m_e$ (N=16 and N=18, see text).
Three different slopes correspond to three pion parameters: $f_\pi = 16\delta$, $m_{\pi^\pm} = 17\delta$ and $\Delta M_\Delta = 18\delta$. Line with the slope m_π=140 MeV=f_π+δ (N=16+1) goes through Λ-, Ξ-, Ω-hyperons and the charmed quark $m_c = 9m_\pi$.
Lines with $\omega-$ and K^*-mesons correspond to stable mass intervals $\Delta M = 2M_q = 6\Delta M_\Delta$, ΔJ=2. Mass of the τ lepton is close to $2m_\mu + 2M''_q$ (top). Stable interval in pseudoscalar mesons is 50δ.

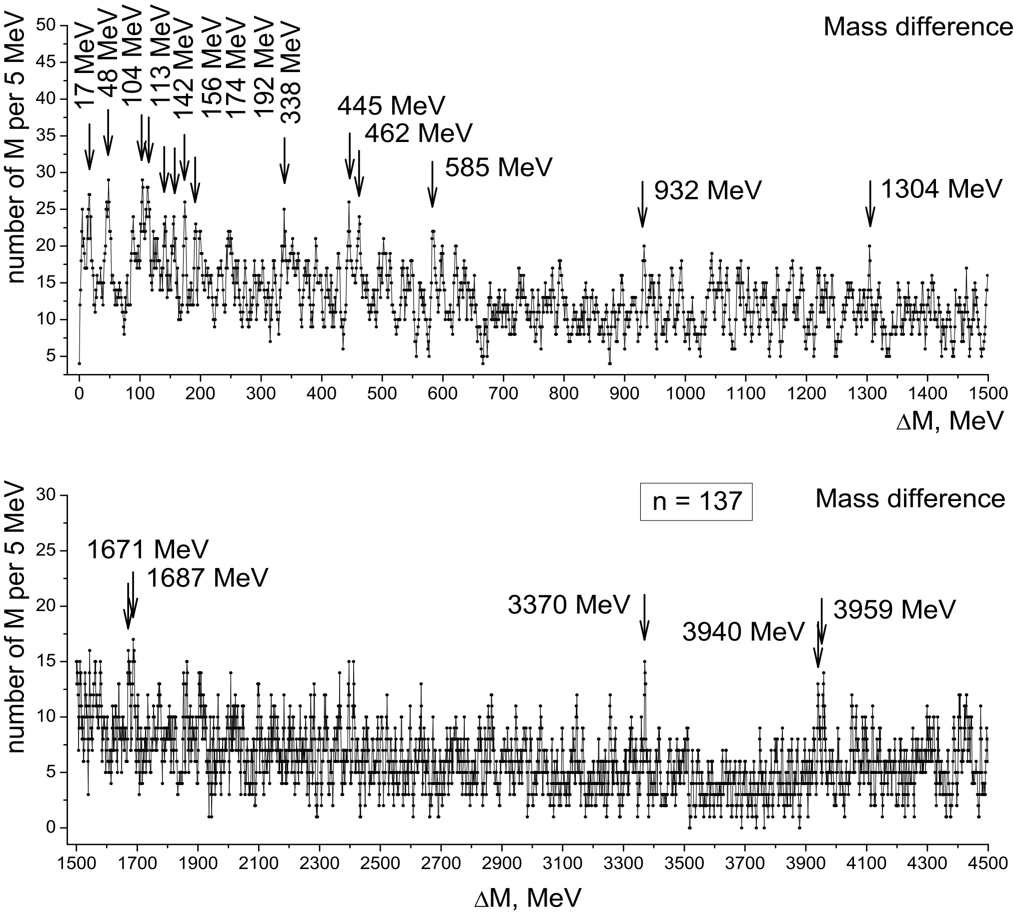

Fig. 2. Distribution of differences between particle masses ΔM in regions 0–1500 MeV–4500 MeV, averaging interval of 5 MeV. Maxima at 16 MeV–48 MeV–104 MeV–141 MeV and doublets at 445–462 MeV, 1671–1687 MeV and 3940–3959 MeV correspond to integers k=2, 6, 13, 17, 54, 12×17 and 9×54 of the period $\delta = 16m_e$ in CODATA relations (2).

The observation of exact integer relation between different parts of expression (2), namely, 16:1 in units m_e and 1:9 in units $(1/8)\delta m_N$, is a very important aspect of the recent state of SM-development. The presence of two systems of fine structures based on two well-known electromagnetic mass differences (periods 170 keV=$m_e/3$ and 161 keV=$\delta m_N/8$) means that such fundamental parameters (which are complimentary to integer numbers of the period $\delta = 16m_e$, common to the particle mass spectrum) should be observed in many effects in nuclear data. A direct reflection of these fine structure intervals can be expected. The fundamental character of QED radiative correction [9,10] and the generally accepted large role of scalar fields, corresponding to the important empirical relation

$$m_e = 3\Delta M_\Delta \cdot (\alpha/2\pi) = 3M_{H^\circ} \cdot (\alpha/2\pi)^2, \tag{3}$$

should be directly observed in nuclear excitation E^* and binding energies E_B (or S_n), as well as in the differences of these nuclear characteristics observed as positions of neutron resonances. The high energy resolution achieved by modern time-of-flight neutron resonance spectrometers can be used to study the fine and superfine structure effects. Existed data on low-lying and highly excited states confirm the CODATA relations. Nuclear spectroscopy has a unique opportunity to contribute to the SM development, based on the CODATA relations and the role of the electron and its symmetry.

2. Superfine structure in neutron resonance spectra

In neutron resonance spectroscopy, the properties of highly excited states are studied with a very high energy resolution, as can be seen in Figs. 3-4, where there are sharp maxima in the position of neutron resonances [14-16,19], and in the D-distributions of the resonances in ^{233}Th, ^{124}Sb, ^{80}Br, ^{104}Rh, ^{105}Pd and ^{179}Hf. The superfine structure in the D-distribution of neutron resonances, noticed by W. Havens [20] in data for Th (Fig. 3, top) with D_{ij}=22 eV=16×ε''=2δ'' in all resonances and D_{ij}=572 eV=1e×4δ'' in strong resonances (*right*) was confirmed by many authors [6,14-16]. The periodicity in the positions of the resonances ^{124}Sb, noticed by K. Ideno (Fig. 3, bottom), is in agreement with the grouping effect in heavy nuclei [19,21-24] (*left*).

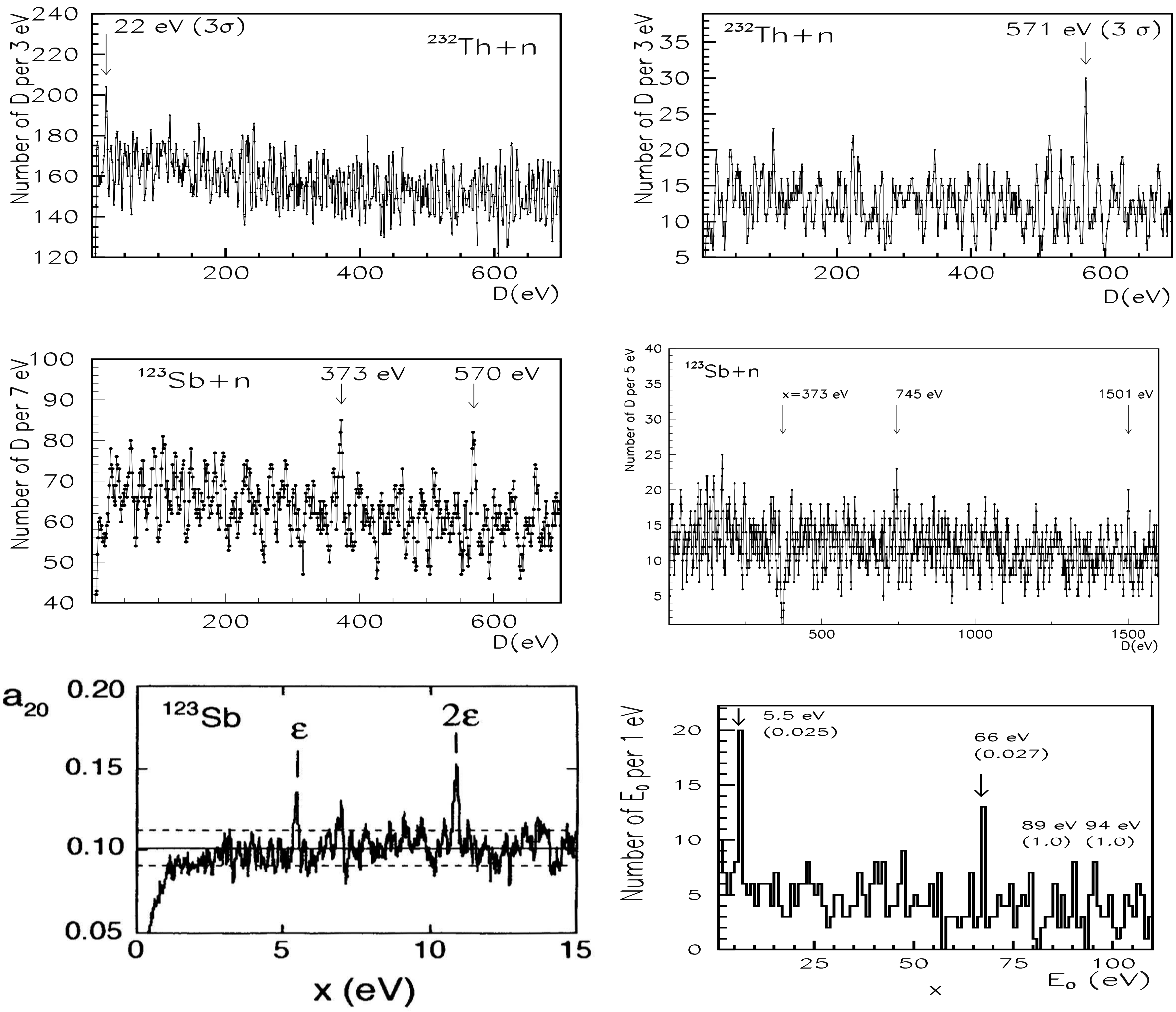

Fig. 3. *Top:* D-distributions of resonances in ^{233}Th (*left*) and the same for resonances with Γ_n° >1 MeV [12]. *Center left:* D-distribution in neutron resonances of the compound nucleus ^{124}Sb. *Center right:* D^{AIM}-distribution for x=373 eV with maxima at 745 eV=4·17δ'' and 1500 eV=8·17δ''. *Bottom left:* The period 5.5 eV in the positions of ^{124}Sb resonances was found by K. Ideno using a special program [23] for analyzing the grouping in resonance positions. *Bottom right:* Distribution of resonance positions known in the 1966 [19]. The selection of one strongest resonance in the interval 10 eV was used (in parentheses is a random probability).

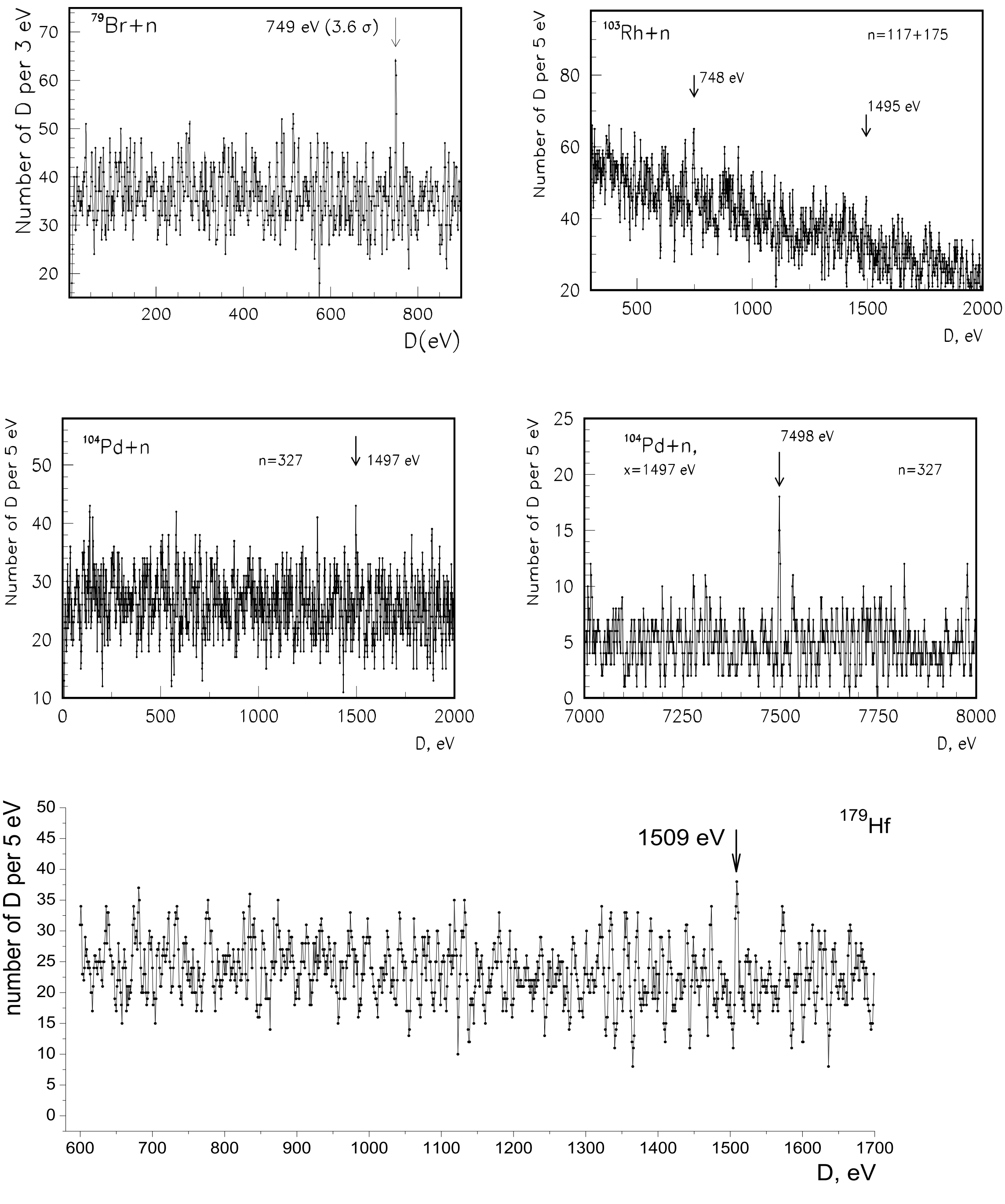

Fig. 4. *Top:* Spacing distribution of neutron resonances in the compound nuclei ^{80}Br (*left*) and ^{104}Rh (*right*), sum of distributions for s- and p-resonances.
Center left: The same for ^{106}Pd.
Center right: D^{AIM}-distribution in ^{106}Pd for x=1497 eV (ratio 7498 eV/1497 eV=5.009).
Bottom: D-distribution in neutron resonances of the compound nuclei ^{179}Hf with maxima at 1509 eV=8·17δ'' (without a small recoil correction A/A+1).

The intervals D^{AIM}=745 eV=17×4δ'' = $2x$ and 1501 eV=17×8δ'' = $4x$ found in ^{124}Sb using the AIM method (Fig. 3) demonstrate the stability of the interval of the superfine structure with N=17 (E_n=$k \cdot \delta''$). The fine structure with k=17 and the ratio $\alpha/2\pi$ between the intervals in neutron resonances and low-lying levels are shown in Table 3.

In Fig. 5 and Table 3 manifestation of the fine structure interval 161 keV=$\delta m_N/8$ = Δ^{TF} is shown as a linear dependence of the excitation energies in the sequence ^{odd}Sb with N=70-82, where the large neutron shell $1h_{11/2}$ is filling in, and the tensor force effect is expected [7,8]. This interval is also observed as a maximum in the sum spacing distribution of ^{122,124}Sb (Fig. 5, top right, 160 keV=17×δ' together with D=530 keV=4×14δ'). The same combination of k=14 and 17 is observed in sum D-distribution for ^{97,98}Pd (Fig. 5).

Table 3. Comparison of excitations E^* (in keV) in Z = 51 A-odd nuclei with integers of Δ^{TF}=161 keV=(δm_N=1293 keV)/8 and close to δm_N intervals in 0$^+$, 2$^+$, 1$^+$ levels of ^{116}Sn.

^{A}Z	^{123}Sb	^{125}Sb	^{127}Sb	^{129}Sb	^{131}Sb	^{133}Sb	^{119}Sb	^{116}Sn	^{116}Sn
(N-70)/2	1	2	3	4	5	6		N=	66
E^*, keV	$\boxed{160.3}$	$\boxed{332.1}$	$\boxed{491.2}$	$\boxed{645.2}$	$\boxed{798.4}$	$\boxed{962.0}$	644	$\boxed{1294}$	$\boxed{1292}$
E^*-$k\frac{\delta m_N}{8}$	$\boxed{-1}$	-9	+7	$\boxed{-1}$	-10	-7	-2	1	-1
$k\frac{\delta m_N}{8}$	161	323	484	646	808	969	646	1293	1293
D, eV		373	570						
ratio D/E^*		114·10^{-5}	116·10^{-5}						

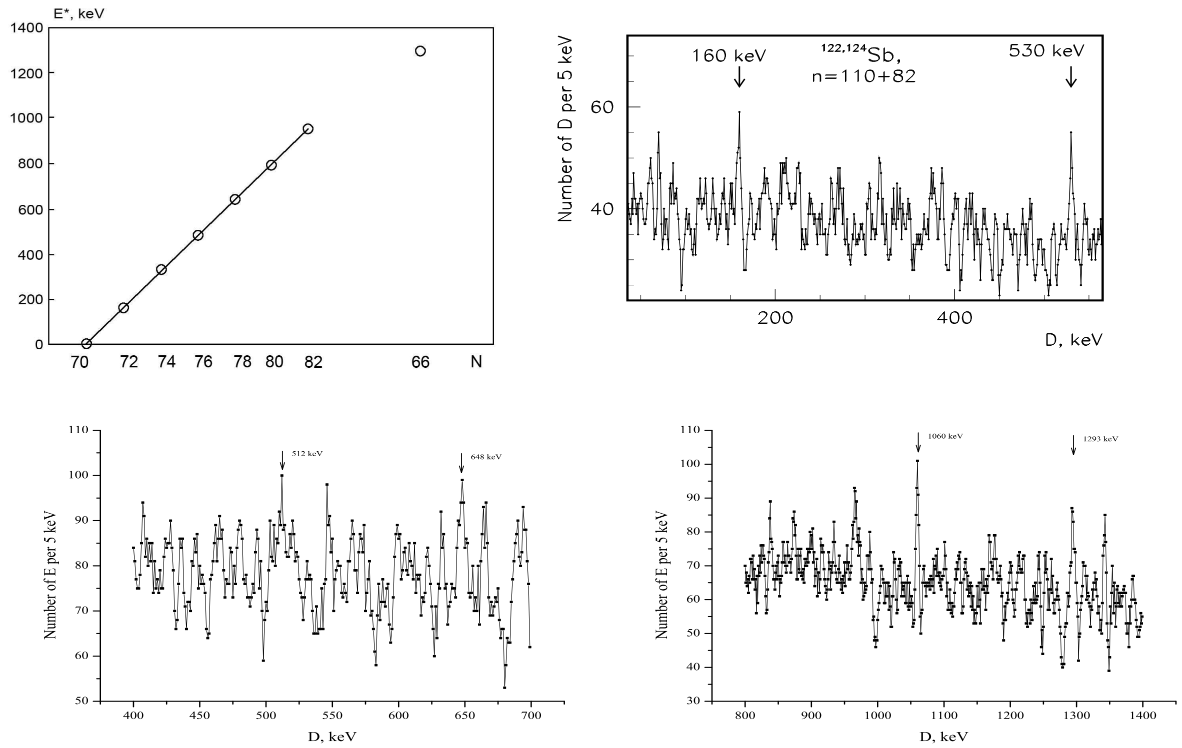

Fig. 5. *Top left*: Linear trend of E^* in ^{odd}Sb with a slope Δ^{TF}=161 keV=$\delta m_N/8$ (Table 2). A point at right corresponds to stable equidistant E^* in ^{116}Sn (J^π=0$^+$, 2$^+$, 1$^+$, boxed at right). *Top right:* Sum D-distribution in low-lying levels ^{122,124}Sb (numbers of states n=110,82). *Bottom*: Sum D-distribution in ^{97,98}Pd in energy region 400-1400 keV. Maxima at 512 keV=m_e = $3 \times 18\delta'$, 648 keV=4×17δ', 1060 keV=$8 \times 14\delta'$ and 1293 keV=$8 \times 17\delta'$ are discussed in the text.

3. Fine structure in neutron resonance spectra

The grouping of the neutron resonance positions in near-magic isotopes with N around 82 with periods $k \times \varepsilon'$=1.16(1) keV and k=1, 4, 8 and 18 are given in Fig. 6 and Table 4 together with the D-distributions of resonances in ^{61}Ni and ^{141}Ce (Fig. 6).

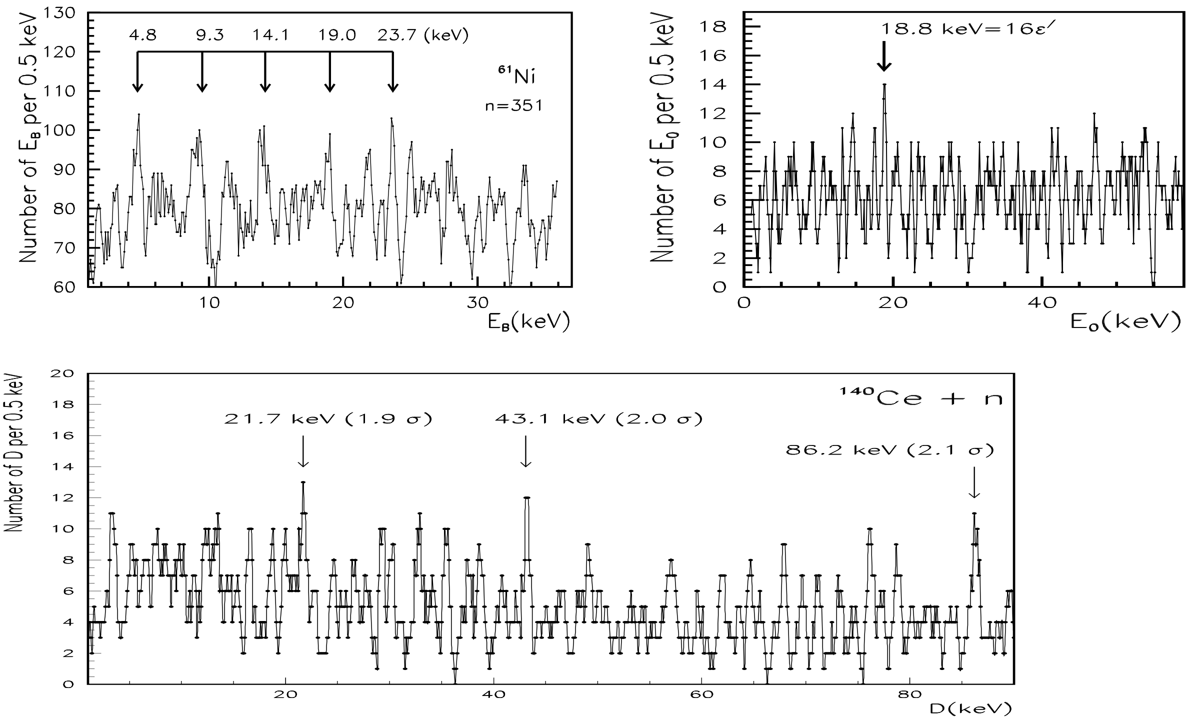

Fig. 6. *Top:* D-distribution of all 351 neutron resonances in the target nucleus ^{60}Ni [14-16]. *Top right:* Distribution of resonance positions in all N-even light nuclei [14-16]. *Bottom:* D-distribution in resonances in ^{141}Ce (period 21.7 keV double-boxed in Table 5).

Table 4. *Top:* Positions of strong neutron resonances in isotopes with N=83 compared with the integer number of the period 9.5 keV=8(ε'=1.188 keV)=δ'. *Bottom:* Positions of strong resonances in isotopes with Z=35-39 compared with $k \times$ (ε'=1.188 keV=9.505 keV/8) (*left*), and excitations E^* ^{143}Ce (boxed are ε'=1.188 keV and 18.9 keV=2δ').

Nucl.	^{141}Ce	^{141}Ce	^{142}Pr	^{141}Ce	^{141}Ce	^{141}Ce	Comments
J_i^π	$1/2^+$	$1/2^+$	$(5/2^-)$				
Γ_n^o,meV	660	3060	160	D	D	D	
E_n	9.573	21.570	9.598	21.7	43.1	86.2	Ratio 9/4
E^*,E_n'	$\boxed{9.505}$	$\boxed{21.418}$	$\boxed{9.530}$				was noticed
$k(8\varepsilon')$	1	9/4	1	9/4	9/2	9	by M.Ohkubo
$k{\times}8\varepsilon'$	$\boxed{9.504}$	21.384	$\boxed{9.504}$	21.4	42.5	85	[22,24]
Nucl.	^{140}La	^{80}Br	^{82}Br	^{86}Rb	^{143}Ce	$J_o^\pi=3/2^-$	
J_i^π	3^+	l_n=0	l_n=0	l_n=0	$7/2^-$	$5/2^-$	
Γ_n^o,meV	54	72.0	120	159	E^*	E^*	
E_n	1.179	1.201	1.209	2.398			
E^*,E_n'	$\boxed{1.170}$	$\boxed{1.186}$	$\boxed{1.194}$	2.370	$\boxed{18.9}$	42.3	
$k(8\varepsilon')$	1/8	1	1	2	2	9/2	
$k{\times}8\varepsilon'$	1.188	1.188	1.188	2.376	19.0	42.77	

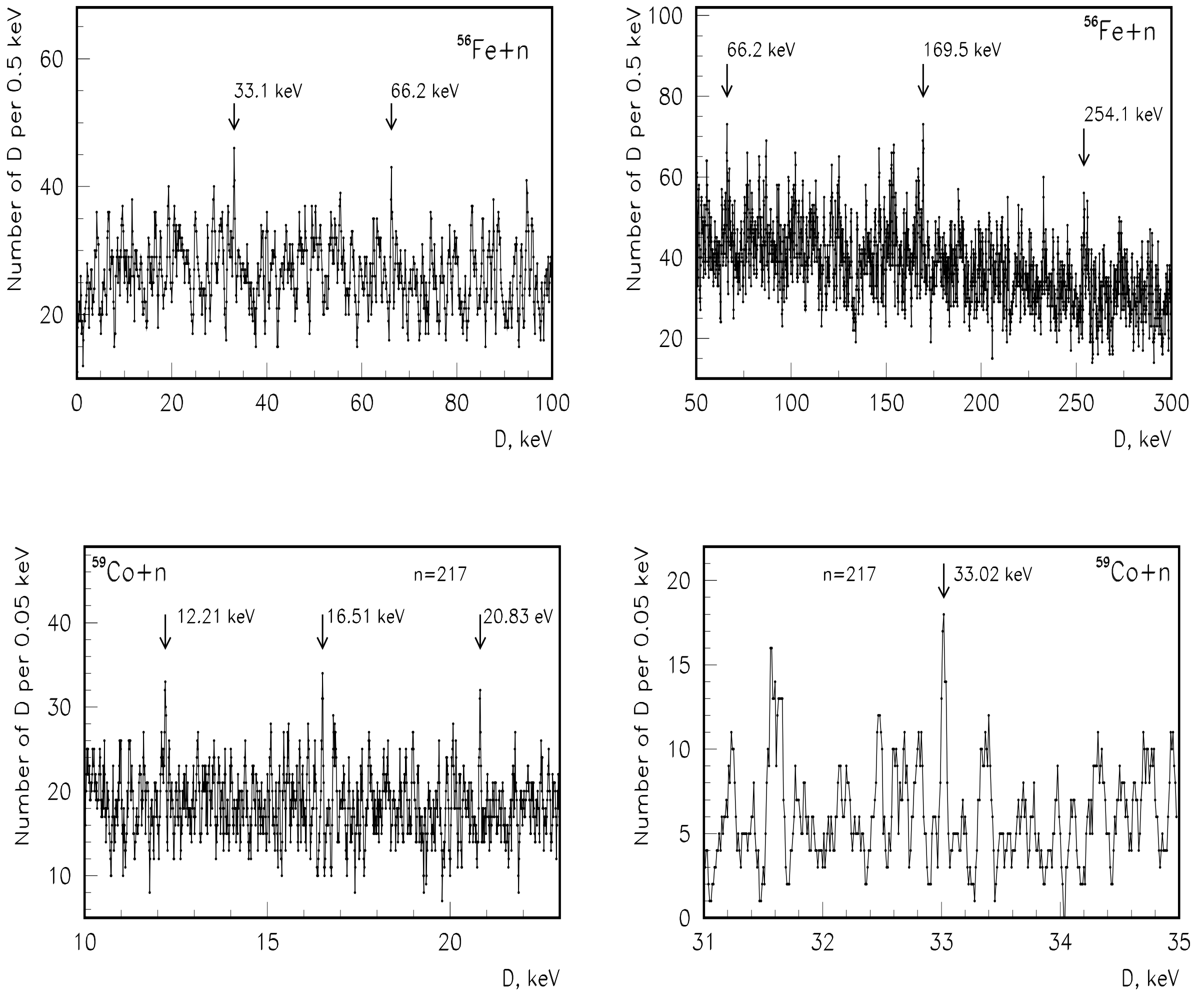

Fig. 7. *Top:* D-distribution in resonances of ^{57}Fe in regions E_n=0-100-300 keV.
Bottom: D-distribution in neutron resonances of ^{60}Co in regions E_n=18-23-35 keV.

D-distributions in the neutron resonances of ^{57}Fe and ^{60}Co in the regions E_n=0-300 keV and E_n=18-35 keV are shown in Fig. 7. The stable interval 33 keV is common for ^{60}Co and ^{57}Fe. In the spacing distribution of all 345 levels of ^{60}Co with the excitation energy E^* smaller than the neutron separation energy S_n (Fig. 9, top), the maxima at D=399 keV=6×66 keV and D=534 keV=8×66 keV correspond to the same system of stable intervals $D = k \times 7\delta'$ observed in the neutron resonance spectrum (Table 5, column n=14). The same fine structure was observed as maxima in the D-distributions in the near-magic Sb and Pd (Fig. 5) and in the sum distribution of excitations of low-lying levels of a broad scope of nuclei with Z=61-73 (exact 1:2 ratio in the positions of the maxima at 531 keV=4×14δ and 1059 keV=8×14δ in Fig. 8, bottom).

The third maximum in this E^*-distribution at 1294 keV=8×17δ coincides with the maximum at 1291 keV in a similar distribution for light nuclei with Z≤29 (Fig. 8, top). Two nearby maxima located at a distance of 144 keV correspond to a shift between 483 keV=3×17δ and 340 keV=2×18δ. Stable excitation with a value of 1024 keV=6×18δ is observed in nuclei with Z=32-37 (center line in Fig. 8). Stable excitation in heavy nuclei (around Z=84) correspond to a maximum close to 683 keV=4×18δ. All these maxima are presented in the top part of Table 5 together with CODATA parameters 161 keV=17δ and 170 keV=1$i\delta$, with the pion parameters and the masses of NRCQM constituent quarks, and the fundamental fields considered in Introduction.

For an independent check of the fine structure with a period of δ' observed in neutron resonances (Figs. 6, 7 and Table 4), and an indirect check of the CODATA relations (2), data on all excitations of light nuclei with Z=20-28 were additionally analyzed [18].

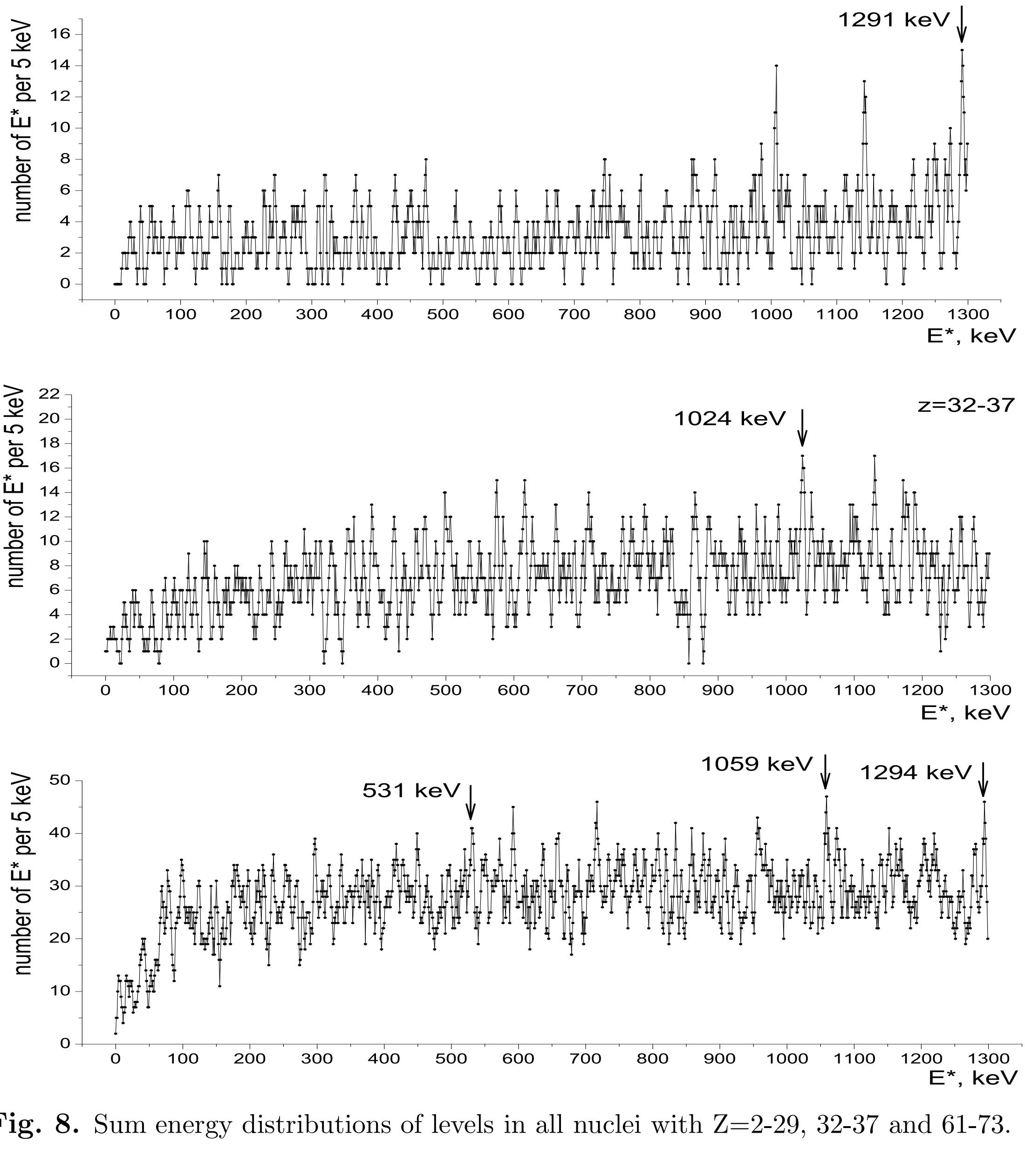

Fig. 8. Sum energy distributions of levels in all nuclei with Z=2-29, 32-37 and 61-73.

Table 5. Stable intervals $D = k \times \mathrm{n} \times 9.5\,\mathrm{keV}$ (n=13, 14, 16, 17, 18, period $\delta' = (\alpha/2\pi)16m_e$) reported in Vol. I/25E L-B Springer, are given together with values found in this work (double-boxed). Boxed in top section are intervals with k=1, n=17, 18 corresponding to the fine structure in nucleon masses (CODATA) and parameters of NRCQM and Standard Model. Values ΣE^* and ΣE_B are sum effects in distributions of nuclear excitation and binding energies obtained for large groups of nuclei [14-16]. Factor $k = 10^3 \approx (\alpha/2\pi)^{-1}$ is considered in [3-6].

k	n=13	n=14	n=16	n=17	n=18
1	CODATA		—	161 keV=$\delta m_N/8$	170 keV=$m_e/3$
8,6	ΣE^*	1059, 531	1212	1291, 1294=δm_N	1024$\approx 2m_e$
10^3	ΣE_B		130 MeV	140 MeV, Λ_{QCD}	147 MeV
10^3	m_μ	NRCQM	$\boxed{f_\pi\text{=131 MeV}}$	$\boxed{m_\pi\text{=140 MeV}}$	$\boxed{\Delta M_\Delta\text{=147 MeV}}$
$3 \cdot 10^3$		NRCQM	$\boxed{M''_q\text{=390 MeV}}$		$\boxed{M_q\text{=441 MeV}}$
10^6	M_Z=91 GeV	SM-param.	M'_H=115 GeV		$\boxed{M_{H^\circ}\text{=125 GeV}}$
1/8-1/2		$\boxed{\boxed{33\ ^{60}\mathrm{Co}}}$	$\boxed{\boxed{19\ ^{51}\mathrm{V},^{53}\mathrm{Mn}}}$		$\boxed{\boxed{21.7\ ^{141}\mathrm{Ce}}}$
1/2		67 ^{40}Ca	76^{46}Sc	82 ^{56}Co $\boxed{\boxed{81\ ^{49}\mathrm{V}}}$	85 ^{65}Cu 85 ^{68}Cu
1/2		$\boxed{\boxed{66\ ^{57}\mathrm{Fe}}}$		$\boxed{\boxed{79\ ^{53}\mathrm{Mn}}}$ Fig. 6	84 ^{55}Co 85 ^{40}Ca
1		$\boxed{\boxed{133\ ^{53}\mathrm{Mn}}}$	151 ^{62}Cu	159 ^{62}Cu	171 ^{63}Cu $\boxed{\boxed{170\ ^{57}\mathrm{Fe}}}$
1,3/2			148 ^{59}Cu	240 ^{66}Cu	251 ^{69}Cu $\boxed{\boxed{254\ ^{57}\mathrm{Fe}}}$
2		265 ^{46}Sc	305 ^{62}Cu	316 ^{56}Co 321 ^{46}Sc	339 ^{64}Cu 338 ^{46}Sc
2				323 ^{40}Ca 322 ^{33}S	341 ^{57}Ni 339 ^{19}F
2,5/2		$\boxed{\boxed{399\ ^{60}\mathrm{C0}}}$ Fig. 9		322 ^{Sc}Sc	340 ^{65}Cu 428 ^{23}Na
3	368 ^{69}Cu	$\boxed{\boxed{399\ ^{49}\mathrm{V}}}$	453 ^{59}Cu		511 ^{42}Ca 514 ^{23}Na
3		$\boxed{\boxed{398\ ^{51}\mathrm{V}}}$			512 ^{55}Co $\boxed{\boxed{511\ ^{49}\mathrm{V}}}$
4	491 ^{46}Sc	$\boxed{\boxed{531\ ^{49}\mathrm{V}}}$		637 ^{22}Na 637 ^{18}F	682 ^{55}Co
4	490 ^{20}F	$\boxed{\boxed{534\ ^{60}\mathrm{Co}}}$ Fig. 9		645 ^{40}Ca 639 ^{65}Cu	
4,5	493,614 ^{18,19}F			646 ^{37}S $\boxed{\boxed{649\ ^{53}\mathrm{Mn}}}$	
6,8	736 ^{42}Ca	$\boxed{\boxed{797\ ^{49}\mathrm{V}}}$	1211 ^{69}Cu	1294 ^{41}K $\boxed{\boxed{1295\ ^{47}\mathrm{V}}}$	$\boxed{\boxed{1017\ ^{53}\mathrm{Mn}}}$
6,8		$\boxed{\boxed{1065\ ^{60}\mathrm{Co}}}$	1204 ^{59}Cu	1292 ^{38}S 1290 ^{53}Mn	$\boxed{\boxed{1021\ ^{49}\mathrm{V}}}$ Fig. 10
8	$\boxed{\boxed{1060\ ^{47}\mathrm{V}}}$		$\boxed{\boxed{1217\ ^{60}\mathrm{Co}}}$	1292 ^{55}Mn 1301 ^{59}Mn	
8-10	1228 ^{19}F			1291 ^{59}Co, 1454 ^{42}Ca	
12	1476 ^{38}Ar	1587 ^{46}Sc		1931 ^{18}F 1943 ^{41}Ca	
12,16	1967 ^{33}S,^{36}Ar			1942 ^{32}Si, 2577 ^{18}F	

4. Fine structure in excitations of nuclei with Z=23,25,27

The results obtained in the additional analysis for isotopes with Z=23, 25, 27 are presented in Figs. 9, 10. In Table 6, where all low-lying levels of ^{60}Co are given, it is shown that in this near-magic nucleus there are many stable intervals in the spectrum (maxima in the spacing distribution for all 345 levels, see Fig. 9, top and center) with energies close to the excitation of low-lying states (a large number (n) of intervals D_{ij}=544, 1005, 1015, 1217 keV in Table 6, bottom). By fixing x at real low-lying excitation levels E^* in the AIM analysis, we check the behavior of these well known E^* (stability of the relations between them) at higher excitation energies. In Fig. 7 (bottom) five intervals close to E^*, demonstrate such an unexpected effect in the case of $x = E^*$=1217 keV in ^{60}Co. Fixing the interval x=1066$\approx 8 \times 14\delta'$ in ^{60}Co (Fig. 9, bottom), we observe in the D^{AIM}-distribution (Fig. 10, top) a maximum at $x/2$=532 keV.

Table 6. Excitations E^* (in keV), J^π and maxima in spacing distribution of ^{60}Co.

E^*	0.0	58.6	277	288	436	506	543	1004	1006	1016	1208	1216	1217
J^π	5^+	2^+	4^+	3^+	5^+	3^+	2^+	(3,4)	4		5^+	6^+	4
D_{ij}		59		288			544		1005	1015			1217
n(D_{ij})							74		73	75			79

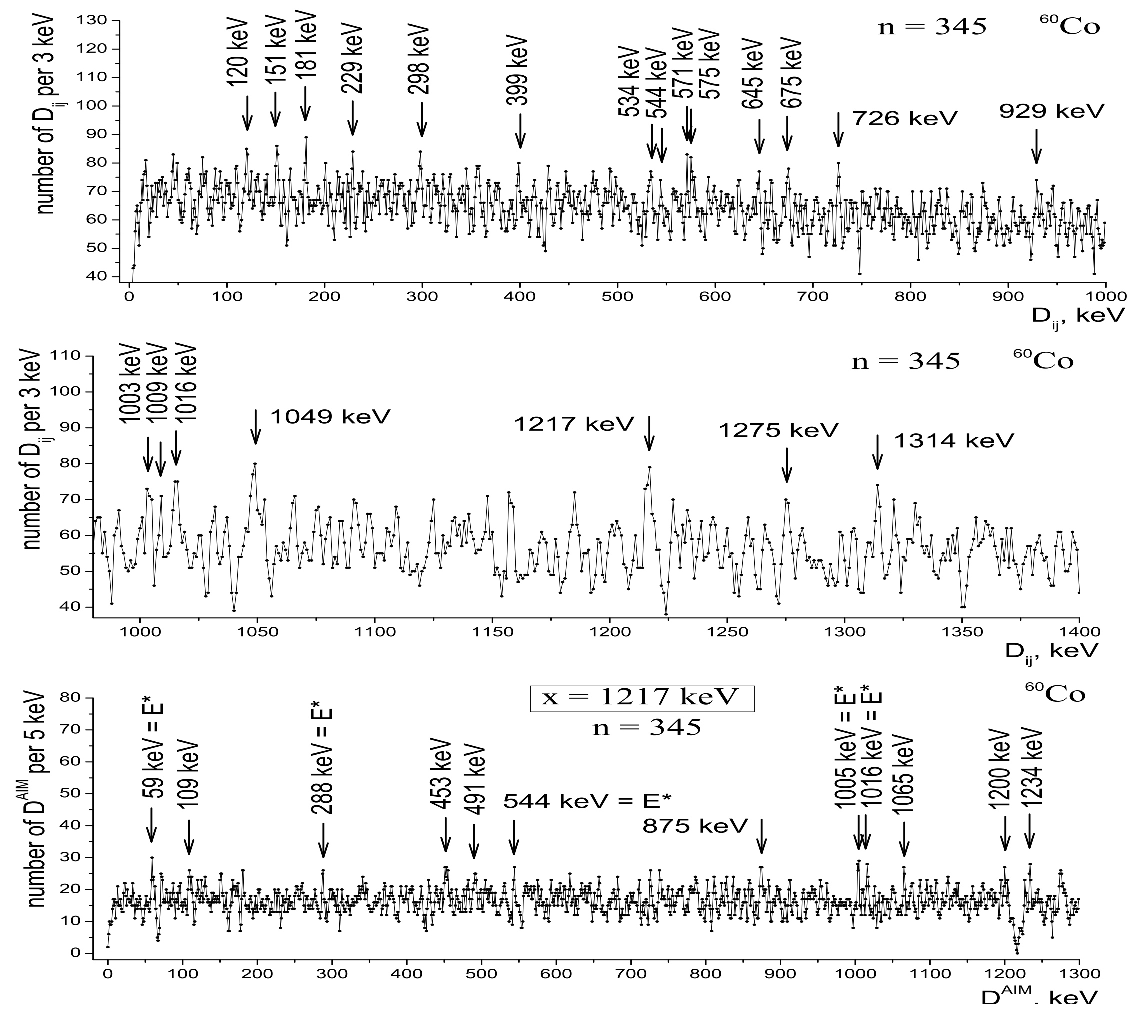

Fig. 9. *Top and center:* Spacing distributions in ^{60}Co for energies 0-1000-1400 keV. *Bottom:* D^{AIM}-distribution for x=1217 keV in ^{60}Co with maxima at excitation energies E^*.

The intervals 1060 keV and 1294 keV=E^* appear together in the ^{47}V spectrum (Fig. 10, center). Similar small intervals 79-81 keV=(17/2)δ' in ^{49}V–^{53}Mn, stable excitations and intervals close to 1293 keV=δm_N are shown in Table 5 (k=17, which also contain the second parameter of the CODATA relations). This means that the presence of fine and superfine structures in nuclear data provides confirmation of the common fundamental dynamics based on the electron.

In the case of ^{49}V, fixing the intervals equal to the low-lying excitation E^*=1021 keV=6×18δ' (Fig. 10, bottom) leads to intervals equal to its half $x/2$=511 keV and $x/2$=339 keV=2×18δ'. Simultaneously, the above considered interval 399 keV (maximum with a deviation of about 6 σ) and the intervals at 531 keV=4×14δ' and at the doubled value D^{AIM}=797 keV=6×δ' confirm the reality of the system of stable intervals 33 keV and 66 keV=14δ', observed in neutron resonance spacing (Fig. 7 and double-boxed values in Table 5). In this table, the results obtained here are presented together with the results considered in Volume I/25E of the Landolt-Boernstein Library, Springer. The interval D=67 keV was assigned to the nucleus ^{40}Ca, located at the beginning of the large subshell $1f_{7/2}$. The results considered here are usually compared with model calculations performed for nucleons in this subshell. Thus, the observed systems of stable intervals can appear in the correlations in the data for all other nuclei with N, Z after 20.

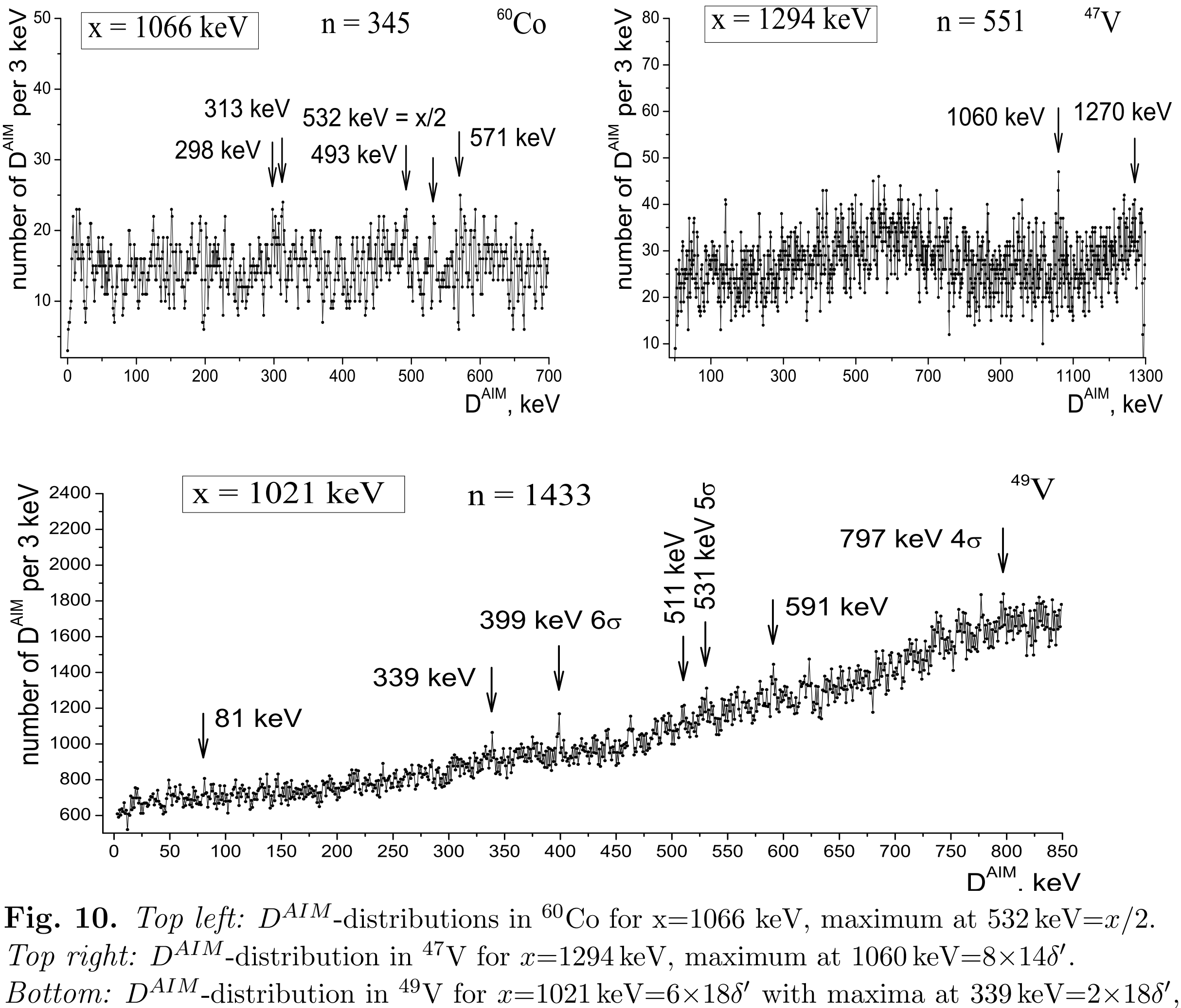

Fig. 10. *Top left:* D^{AIM}-distributions in ^{60}Co for x=1066 keV, maximum at 532 keV=$x/2$. *Top right:* D^{AIM}-distribution in ^{47}V for x=1294 keV, maximum at 1060 keV=8×14δ'. *Bottom:* D^{AIM}-distribution in ^{49}V for x=1021 keV=6×18δ' with maxima at 339 keV=2×18δ', 511 keV=3×18δ', as well as at 399, 541 and 797 keV equal to $k\times 14\delta'$, k=3, 4, 6.

In case of ^{53}Mn, the sum effect of 5 AIM-distributions with different $x = E^*$ (Fig. 11, top) contains strong maxima at 379 keV and 2449 keV, which coincide with a real E^* not included in AIM analysis, and with the maximum at 133 keV=14δ'. In the total spacing distribution of ^{53}Mn (Fig. 11, bottom right), two clearly observed maxima at 10δ'=187 keV and 20δ'=377 keV (ratio 2.02) correspond to k=10 in the same fine structure systematics. The interconnection of this discreteness with the number of protons (n=5) in the shell should be checked.

In both near-magic nuclei with N=28 total spacing distributions (n=546 and 1127 for ^{51}V and ^{53}Mn) contain the same stable value D=19 keV, exactly corresponding to $2\delta = 2\times9.5$ keV, introduced from the grouping of neutron resonances in light and heavy near-magic nuclei (Fig. 6, right, Table 4). An important similarity between the discreteness (δ'=9.5 keV) in nuclear excitations (and the positions of neutron resonances) and the discreteness in CODATA parameters with a period (161 keV+170 keV):(17+18)=9.46 keV should be checked in other nuclear regions.

Analyzes of nuclear spectroscopic data and neutron data were performed separately. It is necessary to avoid inclusion of arrays of resonance energies (in ENSDF) in the analysis of the density of nuclear states. Such a nonstatistical effect from modulation with neutron threshold energies was observed in [25] (the correlation in the separation energies [6] was assigned to E^*).

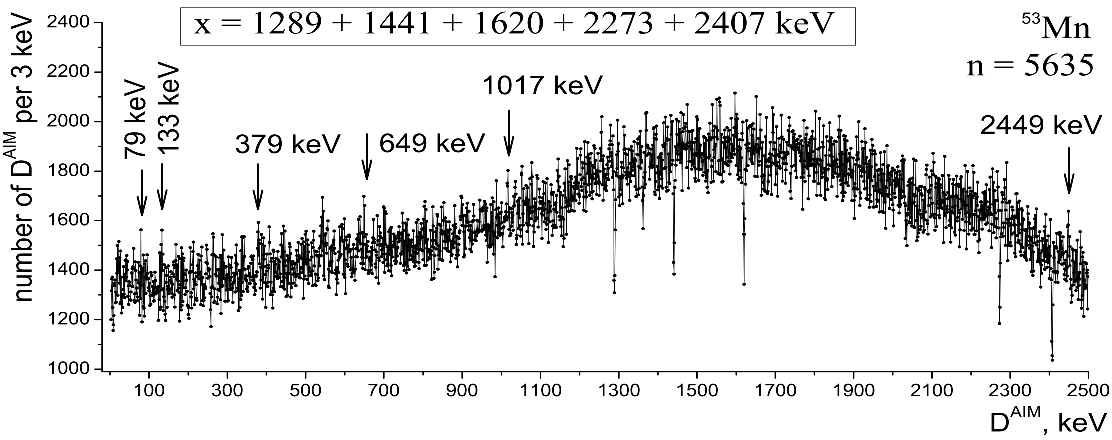

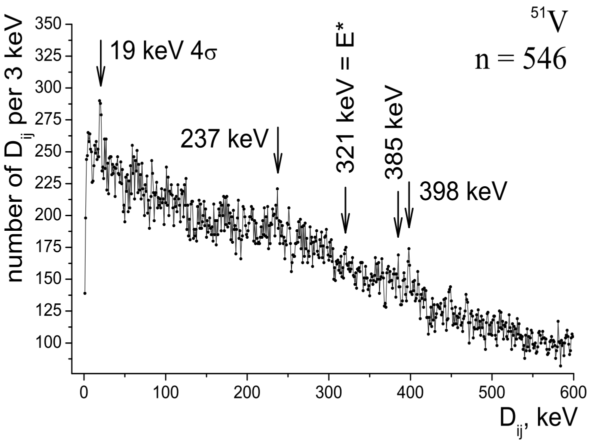

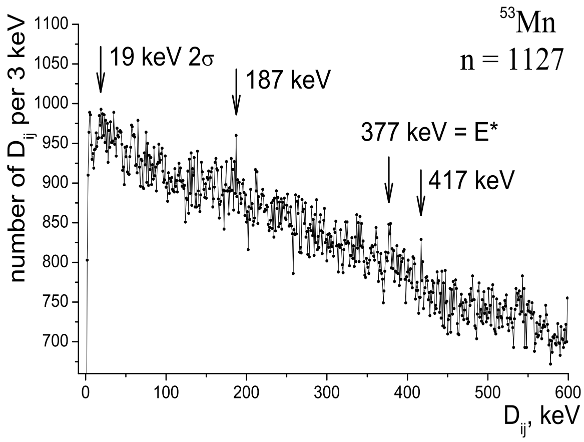

Fig. 11. *Top:* Sum of 5 D^{AIM}-distributions in ^{53}Mn (n=5635=5×1127 for 5 values x). The maxima at E^*=379 keV (5σ) and 2449 keV (6σ), as well as D=79, 133, 649, 1017 keV are marked. 5 strong minima correspond to the positions $x = E^*$ in the AIM analysis.
Bottom left: Spacing distribution in ^{53}Mn, maximum at 19 keV=2δ' (deviation of about 4σ).
Bottom right: Spacing distribution in ^{51}V with maxima at 19 keV=2δ', 187 keV=10δ', 377 keV=20δ'.

5. Conclusions

The analysis of neutron resonances performed here shows the inclusion of the observed fine and superfine structures (in positions and spacing distributions) in the fine structures observed in the charged-particle resonances and in low-lying excitations. The parameters of these common fine structures overlap with the parameters of the fine structure in the particle masses. This means that nuclear data can be used in indirect but independent check of the fundamental properties of matter.

According to F. Wilczek [26], a new aspect of nuclear spectroscopy (”nuclear chemistry” with very accurate results for nuclear states energies) can be used in several important applications, for example, in laser technologies.

Modern nuclear spectroscopy will take part in the unification of interactions based on CODATA relations. For strong interactions, this can be connected with the expression $\alpha_s = 2/17$ (for the distance $1/M_Z$ [2]), which contains a pion mass close to Λ_{QCD}. The particle mass spectrum extends from m_e to the scalar boson mass $M_{H^\circ} = \Delta M_\Delta(\alpha/2\pi)^{-1}{=}(m_e/3)(\alpha/2\pi)^{-2}$ and from the muon mass to the vector boson mass $M_Z = m_\nu(\alpha/2\pi)^{-1}$, which are interconnected by QED corrections and symmetry motivated relations.

The creation of modern nuclear models based on fundamental aspects of nuclear spectroscopic data and neutron resonance data is an important step in the development of the Standard Model.

References

1. M. Tanabashi *et al.* (Part. Data Group), Phys. Rev. D **98** (2018) 030001.
2. P. Mohr, D.B. Newell, B.N. Taylor, Rev. Mod. Phys. **88** (2016) 035009.
3. S.I. Sukhoruchkin, Nucl. Part. Phys. Proc. **300-302** (2018) 75.
4. S.I. Sukhoruchkin, IOP Conf. Series: J. Phys. Conf. Ser. (in press).
5. S.I. Sukhoruchkin, Nucl. Part. Phys. Proc. **294-296** (2018) 129.
6. S.I. Sukhoruchkin, *Statistical Prop. of Nuclei*, ed. G. Garg. Pl. Press, 1972, p. 215.
7. T. Otsuka, T. Suzuku, Y. Utsino, Nucl. Phys. A **805** (2008) 127c.
8. I. Tanihata, Mod. Phys. Lett. A **25** (2010) 1886 (and priv. commun.).
9. R. Feynman, *QED-Strange Theory of Light/Matter*, 1986. Princ. Univ. Press.
10. V.V. Belokurov, D.V. Shirkov, *Theory of Part. Inter.* AIP, 1991; M. Nauka, 1986.
11. Ya.B. Zeldovich, A.D. Sakharov, Yad. Fiz. **4** 1966 395; Sov. J. Nucl. Phys. 4 (1967) 283.
12. C. Itoh *et al.*, Phys. Rev. D **40** (1989) 3660.
13. L.A. Glozman, Nucl. Phys. A **629** (1998) 121c.
14. S. Sukhoruchkin, *Discr. part. masses* Lambert Ac. Publ. 2017. ISBN 978-620-2-02258-3.
15. S.I. Sukhoruchkin, *Proc. LI Winter School of PNPI*, pp. 43–139, SPb., 2018.
16. S.I. Sukhoruchkin, *Proc. L Winter School of PNPI*, pp. 45–119. SPb., 2017.
17. M.H. Mac Gregor, Nuovo Cimento A **103** (1990) 983.
18. S.I. Sukhoruchkin, Z.N. Soroko, D.S. Sukhoruchkin, these Proceedings.
19. S.I. Sukhoruchkin, *Proc. Conf. Nucl. Data for Reactors*, Paris, Vol. 1 , p. 159 (1967).
20. W.W. Havens Jr., *Progr. Fast Neutron Phys.* Univ. Chicago Press, 1963, p. 215.
21. K. Ideno, M. Ohkubo, J. Phys. Soc. Jpn. **30** (1971) 620.
22. M. Ohkubo *et al.*, Rept. JAERIM93112, 1993.
23. K. Ideno, Proc. Conf. Neutr. Research, SPIE Proc. Ser. Vol. **2867**, 1997, p. 398.
24. M. Ohkubo, J. Nucl. Sci. Techn. (Tokyo) **19** (1981) 745.
25. S.L. Saharov, Izv. Rus. Acad. Sci. Phys. **64** (2000) 930; Bull. Rus. Acad. Sci. Phys. **64** (2000) 743.
26. F. Wilczek, Nature **520** (2015) 303.